Opt Quant Electron (2010) 42:69–79
DOI 10.1007/s11082-010-9421-z

Modelling of a simple Dy^{3+} doped chalcogenide glass fibre laser for mid-infrared light generation

S. Sujecki · L. Sójka · E. Bereś-Pawlik · Z. Tang · D. Furniss · A. B. Seddon · T. M. Benson

Received: 2 July 2010 / Accepted: 7 October 2010 / Published online: 22 October 2010

Abstract A simple Dy^{3+}-doped chalcogenide glass fibre laser design for mid-infrared light generation is studied using a one dimensional rate equation model. The fibre laser design employs the concept of cascade lasing. The results obtained demonstrate that efficient cascade lasing may be achieved in practice without the need for fibre grating fabrication, as a sufficient level of feedback for laser action is provided by Fresnel light reflection at chalcogenide glass fibre–air interfaces. Further enhancement of the laser efficiency can be achieved by terminating one of the fibre ends with a mirror. A numerical analysis of the effect of the Dy^{3+} doping concentration and fibre loss on the laser operation shows that with 5 W of pump power, at 1.71 μm wavelength, output powers above 100 mW at ∼ 4.5 μm wavelength can be achieved with Dy^{3+} ion concentrations as low as 3×10^{19} cm^{-3}, when fibre loss is of the order 1dB/m.

Keywords Fibre lasers · Laser modelling · Mid infrared light · Chalcogenide glass fibres

1 Introduction

The mid-infrared (MIR) spectral region, defined as the spectral region 3–25μm, covers important atmospheric windows and molecular fingerprints of numerous gases, liquids and solids as diverse as: greenhouse gases; ground, water and air pollutants; pharmaceuticals; toxic agents; oil, oil products and plastics; biological tissue *etc.*. Here we are concerned with MIR

S. Sujecki (✉) · L. Sójka · Z. Tang · D. Furniss · A. B. Seddon · T. M. Benson
George Green Institute for Electromagnetics Research, The University of Nottingham, University Park, NG7 2RD Nottingham, UK
e-mail: slawomir.sujecki@nottingham.ac.uk

L. Sójka · E. Bereś-Pawlik
Institute of Telecommunications and Acoustics, Wrocław University of Technology, Wybrzeże Wyspiańskiego 27, 50-370 Wrocław, Poland

lasers that cover the wavelength range from 3 to 12 μm, and which have many actual and potential applications in spectroscopic monitoring of such molecular species.

Currently a number of types of sources cover this optical wavelength range, e.g. optical parametric oscillators (OPOs), Frequency Difference Generation (DFG) sources, quantum cascade lasers (QCL) and gas lasers. OPOs use a strong short wavelength pumping laser and a nonlinear crystal to generate a MIR signal. OPOs allow for a large tuning range but are costly, of large foot-print and complex structure. DFG sources on the other hand suffer from low power conversion efficiency and low output power. QCLs have the advantage of a relatively simple and efficient (electrical) pumping mechanism but are not well suited for broadband tuning. Gas lasing (*e.g.* CO at 5.5 μm and CO_2 at 10.6 μm wavelengths) is a mature technology but these lasers are unwieldy and unreliable. (A fairly recent more in depth review of MIR lasers can be found in Ebrahim-Zadeh and Sorokina (2008).

Due to the shortcomings of currently available lasers, the development of solid-state fibre lasers for the MIR wavelength range is desirable. Fibre lasers potentially offer a large tuning range, high output power, good beam quality and relatively large pumping efficiencies. Further, once the technology becomes sufficiently mature for the development of all-fibre devices, MIR fibre lasers offer a compact, robust structure for fibre beam delivery. These advantages taken together make MIR fibre lasers an attractive area for research and development.

One way of realising MIR fibre lasers relies on the development of glass optical fibres doped with active lanthanide ions. In order to implement successfully such technology it is necessary to develop glass hosts which exhibit efficient incorporation of sufficiently high concentrations of lanthanide doping ions with a high efficiency of the optical transitions between the lanthanide ion energy levels. Also the lanthanide doped glass fibres should achieve a low attenuation in the required wavelength ranges. In order to meet these requirements, host glasses with low-phonon energy are prerequisite, e.g. heavy metal oxide, heavy metal halide, chalcogenide or mixed-anion glass matrices. Most recently research has focused on chalcogenide glasses due to: their low phonon energy, high refractive indices (for high cross-sections), relatively good ability to dissolve lanthanide doping ions and development already of sufficiently mechanically and chemically robust passive chalcogenide optical fibres. It is also noted that the low phonon glass technology using lanthanide doping offers also a way for the development of low cost, compact and high beam quality lasers for the visible part of the optical spectrum that could replace the currently available laser sources (Fujimoto et al. 2010).

Over a number of years, significant progress towards the development of lanthanide ion doped MIR fibre lasers with lasing characteristics at least comparable to those offered by OPOs or QCLs has been made (Nostrand 1999; Shaw et al. 2001; Sanghera et al. 2009). One of the main impediments to the development of efficient lanthanide ion doped low phonon energy glass fibre lasers for the MIR wavelength range is that, so far, an efficient 3 or 4 level system for this wavelength range has not been identified.

Prudenzano et al. (2009) have suggested development of Er^{3+} doped photonic crystal fibre lasers and demonstrated their feasibility with conversion efficiency of up to 15% at a fibre loss of 2 dB/m. However, to date, no successful realisation of a lanthanide ion doped photonic crystal fibre of chalcogenide glass has been reported.

A similar performance, but using standard double-clad fibres, has been predicted by Quimby et al. (2008) based on Dy^{3+} doped chalcogenide glasses, to give a 3 level cascade lasing system: $^6H_{11/2}$, $^6H_{13/2}$ and $^6H_{15/2}$ (Fig. 1). A set of two tuned pairs of gratings was part of the design to assist the trapping of idler light at ~3 μm to promote lasing at ~4.5 μm (Fig. 2a). Output powers in the range of hundreds of mWs were predicted, for several

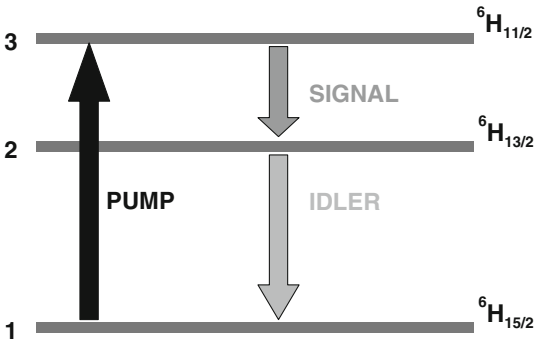

Fig. 1 Dy^{3+} levels for cascade lasing with output signal wavelength of ∼4.5 μm, idler wavelength ∼3 μm and pumping at ∼1.7 μm

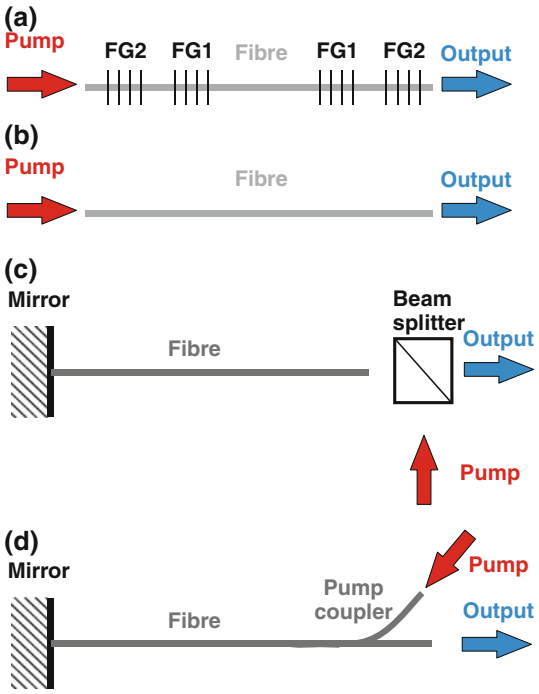

Fig. 2 Cascade laser schemes **a** proposed by Quimby et al. (2008) with fibre Bragg gratings FBG1 and FBG2 tuned to ∼4.5 μm and ∼3 μm, respectively; **b** simple design consisting of the fibre only; **c** an alternative structure with bulk optical elements and **d** an all—fibre structure

Watts of pump power at 1.71 μm wavelength. A large pumping efficiency (∼20%) was anticipated, and a 1 dB/m fibre loss assumed, to give a potentially large continuous tuning range of fibre lasers, when operating in the vicinity of the 4.5 μm output wavelength. Although the results presented (Quimby et al. 2008) clearly demonstrated that a double-clad fibre cascade system may be used for efficient generation of MIR light, the suggested laser structure is still quite challenging in terms of practical realisation requiring the fabrication of two pairs of wavelength-matched fibre gratings in the Dy^{3+}-doped chalcogenide glass fibre. Furthermore, the Dy^{3+}-doped chalcogenide glass fibre simulated as a laser had a large dopant ion concentration (7×10^{19} ions cm^{-3}). In our experience such a fibre is difficult to manufacture because larger concentrations of lanthanide ions may trigger glass devitrification (Tang et al. 2010), with attendant increased fibre loss, decreased fibre robustness and potential spoiling of the emission processes due to possible ion-clustering.

Therefore, in this paper, we explore the feasibility of an alternative laser design (Fig. 2b), which although still based on the 3 level cascade lasing system suggested by Quimby et al. (2008), is more simple because it avoids the use of gratings. The more simple design relies only on the feedback provided by Fresnel reflection at chalcogenide glass- air interfaces, thereby reducing the technological challenge of realising the design. We demonstrate that the efficiency of this simple laser design can be increased to match that of the more complicated design proposed by Quimby et al. (2008) by terminating one fibre end with a mirror (Fig. 2c). The disadvantage of the design depicted in Fig. 2c is the use of bulk optical elements. However, by suitable development of a pump–coupler, this design can, in principle, be converted into an all-fibre laser structure (Fig. 2d).

For the proposed laser structures, we study the dependence of the laser efficiency on the Dy^{3+} doping level and on fibre loss. Such analysis will allow identification of the optimal parameters for fibre laser structures to be realised which are technologically less challenging than that of (Quimby et al. 2008), while still achieving output power levels of 100 mW or above at ~4.5 μm wavelength.

This paper comprises four sections: below in Sect. 2 we present the theoretical model used; in Sect. 3 a numerical analysis of the proposed fibre laser structure is performed, while in the last section we summarise the results.

2 Theory

The three-level model of the Dy^{3+} ion level populations is shown in Fig. 1. Following Quimby et al. (2008), in order to calculate the populations of the three levels, solution of the three associated coupled nonlinear differential equations is necessary. In steady state, these equations can be reduced to form a set of three algebraic equations, which can be represented in the following matrix form:

$$\begin{bmatrix} a_{11} & a_{12} & a_{13} \\ a_{21} & a_{22} & a_{23} \\ 1 & 1 & 1 \end{bmatrix} \times \begin{bmatrix} N_1 \\ N_2 \\ N_3 \end{bmatrix} = \begin{bmatrix} 0 \\ 0 \\ N \end{bmatrix} \tag{1}$$

In (1) the coefficients a_{xx} are as follows: $a_{11} = c_{pa} \times P_p$; $a_{12} = c_{\lambda 1a} \times P(\lambda_1)$; $a_{13} = -c_{pe} \times P_p - c_{\lambda 1e} \times P(\lambda_1) - 1/\tau_3$; $a_{21} = c_{\lambda 2a} \times P(\lambda_2)$; $a_{22} = -c_{\lambda 2e} \times P(\lambda_2) - c_{\lambda 1a} \times P(\lambda_1) - 1/\tau_2$; $a_{23} = c_{\lambda 1e} \times P(\lambda_1) + \beta_{23}/\tau_3$ whereby τ_3 and τ_2 are the lifetimes of level 3 and 2, respectively. β_{32} is the branching ratio for the 3→2 transition. P_p, $P(\lambda_1)$ and $P(\lambda_2)$ are the optical powers for the pump, signal and idler, respectively, at wavelengths λ_1 and λ_2, respectively. The coefficients c_{xy} are expressed by: $c_{pa} = \Gamma_p \sigma_{pa} \lambda_p/(A\ h\ c)$; $c_{pe} = \Gamma_p \sigma_{pe} \lambda_p/(A\ h\ c)$; $c_{\lambda 1a} = \Gamma_{\lambda 1} \sigma_{\lambda 1a} \lambda_1/(A\ h\ c)$; $c_{\lambda 1e} = \Gamma_{\lambda 1} \sigma_{\lambda 1e} \lambda_1/(A\ h\ c)$; $c_{\lambda 2a} = \Gamma_{\lambda 2} \sigma_{\lambda 2a} \lambda_2/(A\ h\ c)$; $c_{\lambda 2e} = \Gamma_{\lambda 2} \sigma_{\lambda 2e} \lambda_2/(A\ h\ c)$, where: A is the doping cross-section; h is Planck's constant; c is the speed of light in free space; Γ_x is the confinement factor and $\sigma_{xya/e}$ is the absorption/emission cross-section for the xy transition. It is noted that in the above formulae, the following standard relationship: $I = \Gamma \times P/A$, was assumed to relate light intensity (I) and power (P) (Becker et al. 1999). Following Quimby et al. (2008) one wavelength is used to represent each of the pump, signal and idler, relying on the assumption that the lasing spectrum within each of the spectral regions is narrow when compared with the rate of the spectral change of the absorption and emission cross sections. This assumption is quite well satisfied even if the corresponding spectra are 1 nm wide.

In a fibre laser, the level populations are modified due to the strong photon densities associated with the optical waves trapped within the laser cavity. The spatial evolution of the

powers for the pump, signal and idler powers are given through solution of the following ordinary differential equations:

$$\frac{dP_p^{\pm}}{dz} = \mp\Gamma_p \left[\sigma_{pa} N_1 - \sigma_{pe} N_3\right] P_p^{\pm} \mp \alpha P_p^{\pm} \tag{2a}$$

$$\frac{dP\,(\lambda_1)^{\pm}}{dz} = \mp\Gamma_{\lambda 1} \left[\sigma_{32a} N_2 - \sigma_{32e} N_3\right] P\,(\lambda_1)^{\pm} \mp \alpha P\,(\lambda_1)^{\pm} \tag{2b}$$

$$\frac{dP\,(\lambda_2)^{\pm}}{dz} = \mp\Gamma_{\lambda 1} \left[\sigma_{21a} N_1 - \sigma_{21e} N_2\right] P\,(\lambda_2)^{\pm} \mp \alpha P\,(\lambda_2)^{\pm} \tag{2c}$$

where '+' and '−' refer to forward and backward travelling waves, $P_p = P_p^+ + P_p^-$; $P(\lambda_1) = P(\lambda_1)^+ + P(\lambda_1)^-$ and $P(\lambda_2) = P(\lambda_2)^+ + P(\lambda_2)^-$.

In order to calculate the output power of the fibre laser for a given value of the pump power, the equations describing the optical power evolution for the pump, signal and the idler (2) and the rare earth ion level populations (1) have to be solved self-consistently. The self-consistent calculation of photon density distributions of the laser cavity modes was performed here by solving equations 1 and 2, subject to boundary conditions at both mirror ends, using the coupled solution method (Sujecki 2007).

3 Fibre laser modelling

In this section, we describe the modelling results obtained for the fibre laser structures presented in Fig. 2 based on using Dy^{3+}:GeAsGaSe chalcogenide glass. The simulation parameters are summarised in Table 1 and were used in all simulations, unless otherwise stated. The absorption spectrum of the pump and fluorescence spectra of the signal and the idler were read from the plots presented in Shaw et al. (2001) and were fitted using Gaussian functions (Desurvire 2002). The respective cross-sectional spectra were then obtained by normalising the absorption and the fluorescence spectra according to the Ladenburg-Fuchtbauer theory (Fowler and Dexter 1962). The shapes of the remaining cross-sectional spectra were obtained from McCumber theory (McCumber 1964) and normalised consistently using the Ladenburg-Fuchtbauer equations (Becker et al. 1999). The missing part of the fluorescence spectrum of the 4.5 μm transition due to CO_2 absorption was extrapolated following Schweizer et al. (1996) as guidance. The emission and absorption cross-section spectra used in the simulations are presented in Fig. 3.

The confinement factor of the pump was estimated assuming a uniform distribution of the pump within a 60 μm diameter. The confinement factor of the signal and idler were estimated by calculating the fundamental mode field distribution at the respective wavelengths. A realistic Fresnel reflection for this type of glass is ~ 20% at each glass–air interface (Savage 1985) and (Dantanarayana et al. 2010) and this is the level of reflection assumed in this paper.

Firstly, we compared the dependence of output power on the pump power for the designs in Fig. 2a–c. The structure shown in Fig. 2a corresponds to the original design of Quimby et al. (2008). The output grating reflectivity for this structure is 0.05 and 0.9 for the signal and the idler, respectively. The discrepancy between our result and the results given by Quimby et al. (2008) is small and can be primarily attributed to using the launched pump power rather than the coupled pump power on the abscissa axis (there is 20% difference between these two values, due to the assumed 20% reflectivity at the chalcogenide glass–air interface). Figure 4 shows that the laser threshold changed by a small amount when using the proposed laser design while the laser slope efficiency was reduced by approximately 50%. However, these

Table 1 Dy^{3+}-doped chalcogenide glass fibre laser modelling parameters

Quantity	Value	Unit
Dy^{3+}-ion concentration	7×10^{19}	cm^{-3}
Core radius	5.5	μm
Numerical aperture	0.2	
Cladding radius	30	μm
Fibre length	2.1	m
Fibre loss at 3 μm wavelength	1	dB/m
Lifetime of level 3	2	ms
Lifetime of level 2	5.2	ms
Branching ratio for 3–2 transitions	0.15	
Output coupler reflectivity for signal (λ_1)	0.2	
Output coupler reflectivity for idler (λ_2)	0.2	
Reflector reflectivity for signal (λ_1)	0.2	
Reflector reflectivity for idler (λ_2)	0.2	
Confinement factor for signal (λ_1)	0.8	
Confinement factor for idler (λ_2)	0.9	
Confinement factor for pump	0.034	
Pump wavelength	1.71	μm
Signal wavelength (λ_2)	4.6	μm
Idler wavelength (λ_2)	3.35	μm

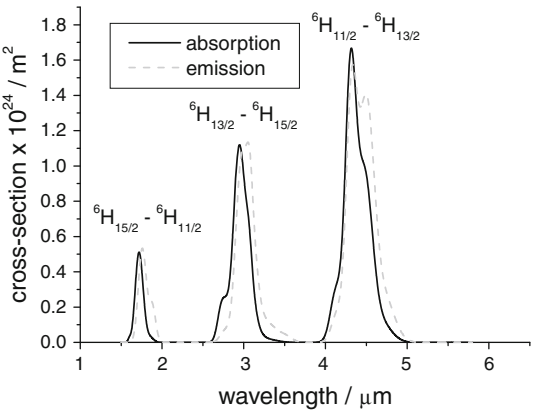

Fig. 3 The spectral dependence of the emission and absorption cross-sections used in the calculations of Sect. 2

results demonstrate also that the output power can be increased by terminating one of the fibre ends with a mirror (Fig. 2c). In such a case, the output power levels then match the ones achieved using the design in Fig. 2a due to Quimby et al. (2008). Another interesting alteration of the original Quimby's design (Fig. 2a) results from inscribing the gratings only at one end of the fibre. Such modification would allow avoiding the need for matching the two pairs of gratings, which is otherwise necessary for the realisation of the design from Fig. 2a. The results from Fig. 4 show that this is a viable alternative, whereby inscribing only the reflector gratings leads to a more efficient operation of the laser when compared with the structure which uses the output coupler gratings only. In comparison with the design from

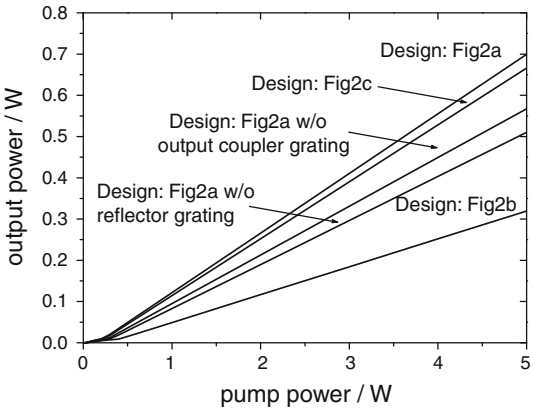

Fig. 4 Calculated dependence of the output signal power on the pump power for the original design due to Quimby et al. (2008) (Fig. 2a) and the proposed designs (Fig. 2b, c). The simulation parameters are given in Table 1

Fig. 2b the modified designs of the original device (Quimby et al. 2008) allow larger output power to be achieved at a given pump power. However, the modified designs are less efficient than the design from Fig. 2c. This latter property results from the fact that the broadband mirror in the design from Fig. 2c does not allow any pump power to leak out at the other fibre end. The penalty for using the broadband mirror is, however, the lack of control over the lasing wavelength.

Figure 5a shows the dependence of the output power on the pump power for selected values of Dy^{3+} doping concentrations for the design from Fig. 2b. In our experience, selenide glasses doped with Dy^{3+} at 7×10^{19} ions cm^{-3} appear to exhibit a large tendency for crystallisation (Tang et al. 2010). It therefore becomes important to explore the dependence of the laser slope efficiency and threshold on the Dy^{3+}-doping level. The results shown in Fig. 5a indicate that, with 5 W of pump power, more than 200 mW of signal power can be achieved if the Dy^{3+}-dopant concentration is at least 5×10^{19} ions cm^{-3}. Further reduction of the Dy^{3+}-dopant concentration significantly quenches the lasing of this fibre laser. Similar suppression of the output signal is observed with increase in fibre loss (Fig. 6a, N.B. the loss was modified for the signal and idler only). Figure 6a shows that even with a fibre loss of 3 dB/m, more than 100 mW of output power can be achieved with 5 W of pump power. The corresponding curves representing the dependence of output power on pump power, for the design from Fig. 2c, are shown for comparison in Figs. 4b and 5b. These results confirm that a large improvement in the laser efficiency can be achieved by the fabrication of an optical mirror at one fibre end. Similarly, the addition of the gratings at one side of the fibre laser allows larger output power to be achieved for a given pump power (Figs. 4c, d, 5c, d).

It should also be noted that by reducing the Dy^{3+}-ion concentration, or increasing fibre loss, the optimal length of the fibre is also affected. Consequently, when using lower Dy^{3+} ion concentrations it is possible to improve the device efficiency over those observed in Figs. 5 and 6 by increasing the fibre length, so long as the fibre loss per unit length is unaffected.

In order to illustrate this point, we calculated the dependence of the output power on fibre length for a fibre laser with Dy^{3+}-doping concentrations of 3×10^{19} and 5×10^{19} cm^{-3}, respectively (Fig. 7). The pump power was set to 5 W. The results from Fig. 7 show that by increasing the fibre length, the output power can be increased. A particular improvement is observed for a dopant concentration of 3×10^{19} cm^{-3}. The results shown in Fig. 7 indicate that on increasing fibre length to 5 m, the output power can be increased to >100 mW.

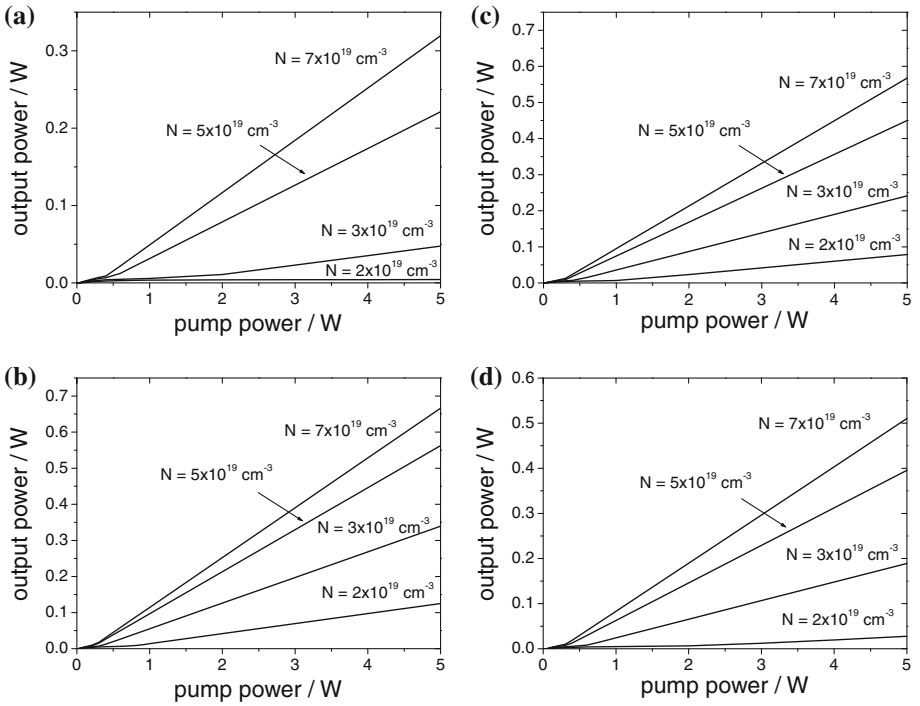

Fig. 5 Calculated dependence of the output signal power on the pump power for the design from Fig. 2b (**a**), Fig. 2c (**b**), Fig. 2a without the output coupler grating (**c**) and Fig. 2a without the reflector grating (**d**) at selected values of Dy^{3+}-ion concentration. The simulation parameters are given in Table 1

However, for larger fibre lengths, the laser output power starts to decrease due to the combined effect of pump depletion through the transfer of pump power to the signal and idler and due to the cumulative fibre loss.

Importantly, we note that by removing gratings from the fibre laser design of Quimby et al. (2008) the mechanism of selecting the wavelength of the idler wave is removed. Although a mechanism for selecting the idler wavelength could be introduced also in the design in Fig. 2b by injection locking, this would complicate the laser structure. Therefore in Fig. 8 we model the dependence of the signal and idler output power on the idler wavelength. It is expected that without spectrally selective feedback, due to mode competition the idler wavelength will settle at a value corresponding to the largest effective round trip gain and, consequently, also to the largest idler output power (and internal cavity photon density), which according to published data on the emission and absorption cross sections implies that the wavelength is approximately within the range between 3,100 and 3,200 nm. This range of wavelengths is very near to the optimal wavelength for the idler, which should be on the long wavelength side of the $^6H_{13/2}$-$^6H_{15/2}$ transition (Quimby et al. 2008). In order to explore further the effect of the detuning of the idler wavelength from the optimal value we calculated the dependence of the output power for the signal and the idler on the idler wavelength within the range from 2.95 to 3.55 μm. It is noted that outside of this range the idler is suppressed due to either the low value of the emission and absorption cross-sections or due to the absorption cross-section being larger than the emission cross-section.

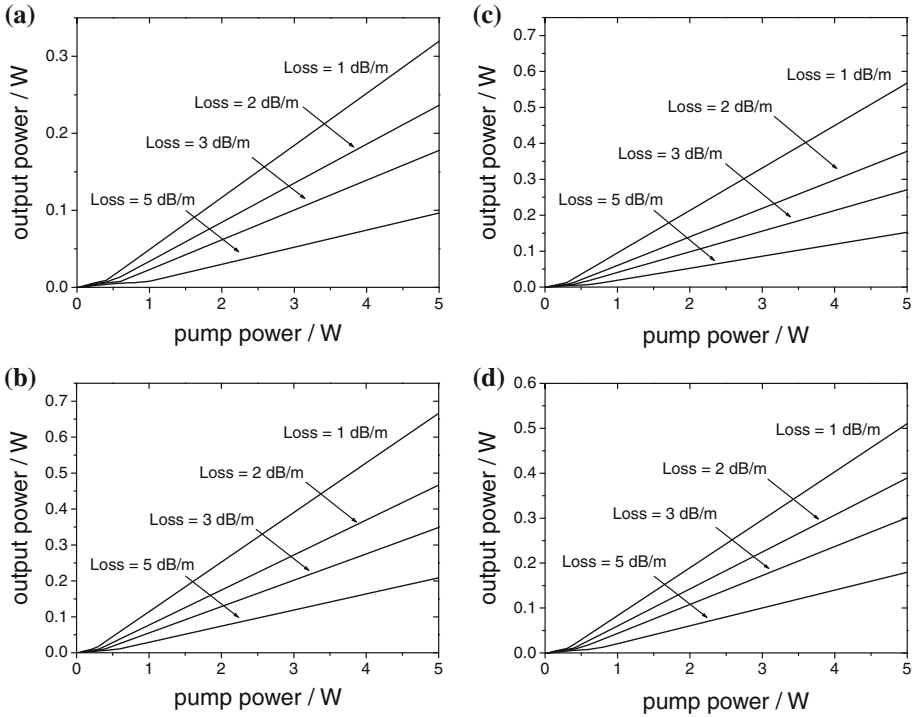

Fig. 6 Calculated dependence of the output signal power on the pump power for the design from Fig. 2b (**a**), Fig. 2c (**b**), Fig. 2a without the output coupler grating (**c**) and Fig. 2a without the reflector grating (**d**) at selected values of fibre loss. The simulation parameters are given in Table 1

Fig. 7 Calculated dependence of the output signal power on the fibre length for the design from Fig. 2b at selected values Dy^{3+}-ion concentration and the launched pump power equal to 5 W. The simulation parameters are given in Table 1

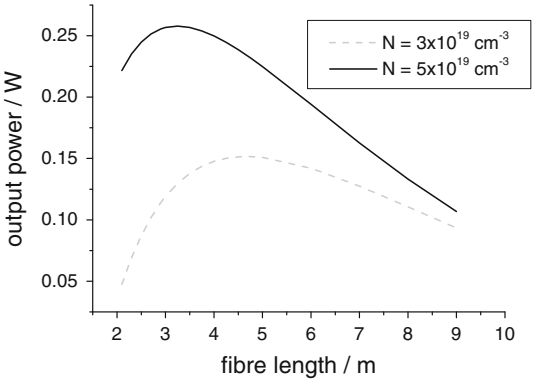

The results from Fig. 8 show that the penalty imposed onto the output power by moving the idler wavelength between 3,050 and 3,450 nm is moderate and does not preclude a successful realisation of an efficient MIR fibre laser operating near 4,500 nm. Therefore it is concluded that fixing the idler wavelength by using gratings or by injection locking is not necessary although using a well tuned grating or injection locking would allow for achieving the maximum output power for the signal wave.

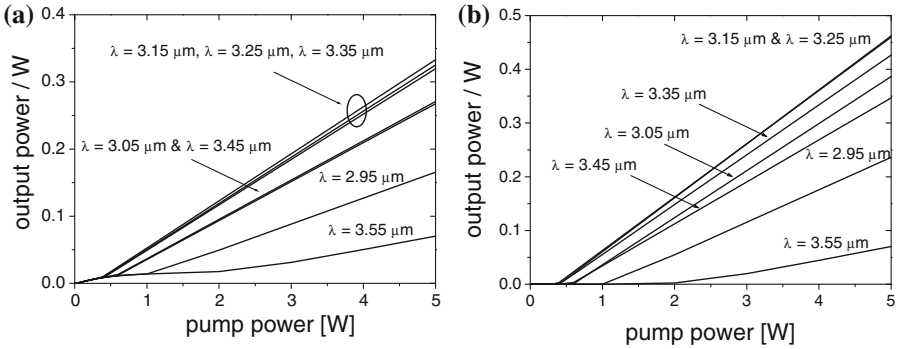

Fig. 8 Calculated dependence of the output signal power (**a**) and the idler output power (**b**) on the pump power for selected values of idler wavelength. The simulation parameters are given in Table 1

As a final comment, it is noted that the proposed design can be used to generate 3 μm light as efficiently as 4.5 μm, which might be useful for developing IR dual wavelength sources.

4 Conclusions

In this paper we have considered a simple fibre laser design, to avoid fabricating fibre gratings in Dy^{3+}-doped chalcogenide glass fibres. The proposed device relies on Fresnel reflection at the chalcogenide fibre glass–air interfaces. The results obtained confirm that a 50% reduction of laser efficiency is to be expected, when compared with a device using fibre gratings. However, this loss in efficiency can be compensated by terminating one fibre end with an optical mirror. The results also confirm that for efficient operation of cascade lasing in Dy^{3+}-doped chalcogenide fibre, fixing of the idler wavelength by means of an optical grating is not necessary though helpful in maximising the output power. Finally, the numerical results show that using a singlemode, double-clad, fibre laser with 5 W of pump power at 1.71 μm wavelength, then output powers above 100 mW at ∼4.5 μm wavelength may be achieved with Dy^3-ion concentrations as low as 3×10^{19} cm^{-3}, hence minimising the risk of the glass devitrification, when fibre loss is of the order 1 dB/m.

References

Becker, P.C., Olsson, N.A., Simpson, J.R.: Erbium Doped Fibre Amplifiers. Academic Press, San Diego (1999)

Dantanarayana, H.G., Vukovic, A., Sewell, P., Lian, Z.G., Furniss, D., Seddon, A.B., Romanova, E.A., Konyukhov, A., Derkowska, B., Orava, J., Wägner, T., Benson, T.M.: The Optical Properties of Chalcogenide Glasses: From Measurement to Electromagnetic Simulation Tools. To be published in ICTON 2010 IEEE Proceedings

Desurvire, E.: Erbium-doped Fiber Amplifiers: Principles and Applications. Wiley, New Jersey (2002)

Ebrahim-Zadeh, M., Sorokina, I.T. (eds.): Mid-infrared Coherent Sources and Applications, NATO Science for Peace and Security Series B: Physics and Biophysics. Springer, The Netherlands (2008)

Fowler, W.B., Dexter, D.L.: Relation between absorption and emission probabilities in luminescent centers in ionic solids. Phys. Rev. **128**(5), 2154–2165 (1962)

Fujimoto, Y., Ishii, O., Yamazaki, M.: Yellow laser oscillation in Dy^{3+}-doped waterproof fluoro-aluminate glass fibre pumped by 398.8 nm GaN laser diodes. Electron Lett. **46**(8), 586–587 (2010)

McCumber, D.E.: Einstein relations connecting broadband emission and absorption spectra. Phys. Rev. **136**(4A), A954–A957 (1964)

Nostrand, M.C., Page, H.R., Payne, S.A., Krupke, W.F.: Room-temperature laser action at 4.3–4.4 μm in $CaGa_2S_4$:Dy^{3+}. Opt. Lett. **24**, 1215–1217 (1999)

Prudenzano, F., Mescia, L., Allegretti, L.A., De Sario, M., Palmisano, T., Smektala, F., Moizan, V., Nazabal, V., Troles, J.: Design of Er^{3+}-doped chalcogenide glass laser for MID-IR application. J. Non-Crystal. Solids **335**, 1145–1148 (2009)

Quimby, R.S., Shaw, L.B., Sanghera, J.S., Aggrawal, I.D.: Modeling of cascade lasing in Dy: Chalcogenide glass fiber laser with efficient output at 4.5 μm. IEEE Photon. Technol. Lett. **20**, 123–125 (2008)

Sanghera, J.S., Shaw, L.B., Aggrawal, I.D.: Chalcogenide glass-fiber-based mid-IR sources and applications. IEEE J. Selected Topics Quantum Electron. **15**, 114–119 (2009)

Shaw, L.B., Cole, B., Thielen, P.A., Sanghera, J.S., Aggrawal, I.D.: Mid-wave IR long-wave IR laser potential of rear-earth doped chalcogenide glass fiber. IEEE J. Quantum Electron. **48**, 1127–1137 (2001)

Schweizer, T., Hewak, D.W., Samson, B.N., Payne, D.N.: Spectroscopic data of the 1.8-, 2.9- and 4.3- mm transitions in dysprosium-doped gallium lanthanum sulphide glass. Opt. Lett. **21**, 1954–1956 (1996)

Savage, J.A.: Infrared optical materials and their antireflection coatings. Adam Hilger Ltd, Bristol, ISBN 0-85274-790-X (1985)

Sujecki, S.: Stability of steady state high power semiconductor laser models. J. Opt. Soc. Am. B **24**, 1053–1060 (2007)

Tang, T., Neate, N.C., Furniss, D., Sujecki, S., Benson, T.M., Seddon, A.B.: Crystallisation behaviour of Dy^{3+}-doped selenide glasses. To be published in Journal of Non-Crystalline Solids, Proc. International Symposium of Non-Oxide and New Optical Glasses, Ningbo, China (2010)